JOURNAL OF GUIDANCE, CONTROL, AND DYNAMICS
Vol. 25, No. 1, January–February 2002

Optimal, Low-Thrust Earth-Orbit Transfers Using Higher-Order Collocation Methods

Albert L. Herman*
Spectrum Astro, Inc., Gilbert, Arizona 85233
and
David B. Spencer†
Pennsylvania State University, University Park, Pennsylvania 16802

A trajectory optimization technique based upon higher-order collocation is used to solve optimal, low-thrust, Earth-orbit transfer problems. The optimal control problem solved is defined, and the solution method for solving this problem is described. For several example cases analyzed, a spacecraft is transferred from low Earth orbit to a variety of final mission orbits. A range of thrust accelerations from approximately 1 to 10^{-3} g was used. A comparison is made between the optimal transfers found in this work and the transfers found by using analytical blended control methods. Finally, conclusions drawn from this work are discussed.

Nomenclature

a	=	semimajor axis
$a, e, i, \Omega, \omega, \nu, M$	=	modified classical orbital elements
c	=	effective exhaust velocity
e	=	eccentricity
$\boldsymbol{f}(\boldsymbol{x}, \boldsymbol{u}, t)$	=	$n \times 1$ vector of system dynamical equations
i	=	inclination
$\tilde{J}$	=	performance function
L	=	true longitude
M	=	mean anomaly
p	=	semilatus rectum
p, f, g, h, k, L	=	modified equinoctial orbital elements
r_a	=	apogee radius
T	=	thrust magnitude
$\boldsymbol{T}$	=	thrust vector
T/m_0	=	initial thrust acceleration
t	=	time
$\boldsymbol{u}$	=	$m \times 1$ control vector
$\boldsymbol{x}$	=	$n \times 1$ state vector
α	=	in-plane thrust angle
β	=	out-of-plane thrust angle
Δ_n	=	normal component of thrust acceleration vector
Δ_r	=	radial component of thrust acceleration vector
Δ_θ	=	tangential component of thrust acceleration vector
Δt_i	=	burn duration for burn i
ΔV_{eff}	=	effective delta V
η	=	ratio of mass to initial mass, m/m_0
μ	=	gravitational constant
ν	=	true anomaly
ϕ	=	scalar performance function
$\boldsymbol{\Psi}$	=	$q \times 1$ vector of desired final conditions of the states
Ω	=	right ascension of the ascending node
ω	=	argument of periapsis

Subscripts

F	=	final
I	=	initial
L	=	final increment of grid
O	=	initial increment of grid

Presented as Paper AAS 99-408 at the AAS/AIAA Astrodynamics Specialists Conference, Girdwood, AK, 16–19 August 1999; received 5 June 2000; revision received 11 September 2001; accepted for publication 13 September 2001.

*Principal Engineer, Mission Analysis and Simulation; albert.herman@specastro.com. Senior Member AIAA.
†Assistant Professor of Aerospace Engineering; dbs9@psu.edu. Associate Fellow AIAA.

Introduction

FOR several decades advanced propulsion technologies have been investigated and developed for use in space. These new systems bring a promise of greatly increased propellant efficiencies, an order of magnitude or greater than systems currently in wide use. With the use of these new propulsion technologies, spacecraft developers will soon place space systems in Earth orbit with considerable greater capabilities. These new space systems might be designed with much larger payloads or, alternatively, significantly greater lifetimes.

This new propulsion technology achieves very high specific impulse values in the range of a few thousand seconds while having relatively low-thrust levels, typically characterized in units of milliNewtons. Because of the low-thrust levels, these new propulsion systems might be required to operate for extended periods during orbit transfers, perhaps for the entire transfer, in order to achieve the required mission orbit. Software for solving orbit transfer problems using low-thrust propulsion must model the dynamics of a transfer adequately to develop solutions that are accurate enough to support advanced mission studies and flight operations.

During the past decades, several researchers have analyzed low-thrust orbit transfer problems. In the 1960s many studied the utility of a solar-electric transfer vehicle. This spacecraft used solar-electric panels to power an electric (ion or arcjet) engine. The thrust level developed for such an orbital transfer vehicle was very small (on the order of thousandths to hundredths of a g). The typical orbit transfer took a very long time, with the transfer trajectory resembling a spiral. Dickerson and Smith[1] derived the necessary conditions required for optimal solar-electric-powered flight, using the calculus of variations techniques from classical optimization theory. Sauer[2] proposed developing a solar-electric propulsion planetary orbiter spacecraft. He found that the use of this type of spacecraft (based on 1960s technology) could deliver to Mars a significantly larger payload than conventional rockets. Additionally, using a chemical rocket to escape Earth, he found that there was only a 15% increase in transfer time from Earth to Mars.

In the 1970s NASA embarked on their Solar Electric Propulsion Stage program. The significant problem associated with the trajectory optimization problem, as found by Oglevie et al.,[3] was that of maintaining the optimal path while pointing the solar arrays (within tolerances) at the sun. In the late 1980s the U.S. Air Force began a

program entitled ELITE (ELectric Insertion Transfer Experiment), in which the objective is to build, test, and fly a solar-electric orbit transfer and orbit maneuvering vehicle, as a precursor to an operational electric orbit transfer vehicle.[4] Both of these programs face the problem of extended operations in a transfer orbit, which is one of the many factors that must be incorporated into design trade studies.

Many authors have studied the trajectory optimization problem associated with the low-thrust propulsion systems. Brusch and Vincent[5] found multiple transfers between specific initial and final orbits, for both optimal and nonoptimal transfer trajectories. Edelbaum[6] used a method of averaging that allows quicker trajectory evaluation than methods based upon numerical integration of differential equations. His method was used for a solar-powered spacecraft that included a model for solar-cell degradation of power. Redding[7] used Lawden's "primer vector" theory to analyze impulsive and near-impulsive transfers for prediction of the initial conditions for low-thrust transfers. In his work algebraic approximations for total time and gravity loss are presented, which are valid for relatively efficient transfers. Redding also showed that gravity losses for a transfer could be reduced to a low level if enough burns are done, irrespective of the thrust levels. Alfano[8] considered the continuous thrust, minimum time transfer, where he used two timescales (fast and slow) to determine small changes in orbital elements for a single revolution and many revolutions, respectively. Bauer[9] found a near-optimal, low-thrust spiral transfer, where the eccentricity remains near zero during the entire transfer. Stewart and Melton[10] presented a multivariable perturbation solution using a fixed steering law and found a relatively low error when compared with the numerical solution. Hargraves and Paris[11] first used direct methods for trajectory optimization. Their implicit integration scheme is based on using a Hermite interpretation to convert the optimal control problem into a nonlinear control problem that includes such things as constraints, discontinuities, and control inequalities. Spencer[12] and Herman[13] give more information on past work.

In this paper the optimal control problem solved during this work is defined, and the solution method for solving this problem is described. Analyses of several Earth-orbit transfer problems are described. These problems include a range of thrust levels and final orbits achieved to demonstrate the flexibility of the methodology developed. This solution method is used to verify the capability of an alternative solution method, which is based upon a simplified thrusting profile and heuristics to achieve the desired orbit. Finally, conclusions drawn from this work are given.

Optimal Control Problem

In this work the control histories that take a set of states from specified initial conditions to their desired final conditions are determined, while minimizing a function of the final values of the states and/or time. These states are governed by a system of first-order, ordinary differential equations given in Eq. (1) by

$$\dot{\boldsymbol{x}} = \boldsymbol{f}(\boldsymbol{x}, \boldsymbol{u}, t) \tag{1}$$

The initial conditions for the states are

$$\boldsymbol{x}(t_I) = \boldsymbol{x}_I \tag{2}$$

The desired final conditions are represented by

$$\boldsymbol{\Psi}[\boldsymbol{x}(t_F)] = \boldsymbol{0} \tag{3}$$

The control time histories are to be chosen such that a performance function given by

$$\tilde{J} = \phi[\boldsymbol{x}(t_F), t_I, t_F] \tag{4}$$

a scalar function of the values of the states at the final time and the initial and final times, is minimized while satisfying the system differential equations given in Eq. (1) with initial conditions given in Eq. (2) and final condition constraints given in Eq. (3). Bryson[14] and Bryson and Ho[15] provide excellent presentations on developing an optimal control formulation that results in an indirect formulation. Kechichian,[16] among others, provides an excellent reference on indirect methods for low-thrust Earth-orbit transfers. In this work a method of solving for the controls directly is used and described in the next section.

Solution Method

In the direct method the problem is transformed into a mathematical programming (MP) problem. This transformation is performed by first discretizing the solution time history and then applying an approximate integration method. This approach begins with the discretization of the solution time history into L subintervals, not necessarily of equal length. The endpoints of these subintervals are denoted as $\{t_0, t_1, \ldots, t_{i-1}, t_i, t_{i+1}, \ldots, t_{L-1}, t_L\}$. Within a given subinterval $[t_{i-1}, t_i]$ the time history of a solution is approximated by a numerical integration of the system dynamics, Eq. (1). Information on the Higher Order Collocation 7th degree system (designated as HOC7) derivation is found in Herman.[13]

We have formulated the original optimal control problem as a mathematical programming (MP) problem where the controls are determined to minimize the performance function given in Eq. (4) directly. In this MP, HOC7 constraints are applied to solving the system differential equations given in Eq. (1), resulting in a nonlinear programming (NLP) problem where the constraint Jacobian exhibits a high degree of data sparseness. For this work the software package SNOPT[17] is used to solve the NLP-formulated problem. This package was chosen because of its appropriateness for sparse matrix problems. The resulting method is called direct HOC7 or DHOC7.

Modified Equinoctial Orbit Elements

To model a transfer trajectory, modified equinoctial orbit elements are used to describe orbit transfers in order to avoid the singularities that occur in the modified classical orbit elements $(a, e, i, \Omega, \omega, M)$, when $e = 0$ and $i = 0$ deg. The modified equinoctial orbit elements (p, f, g, h, k, L) are defined in terms of the modified classical orbital elements as

$$p = a(1 - e^2) \tag{5}$$

$$f = e\cos(\omega + \Omega) \tag{6}$$

$$g = e\sin(\omega + \Omega) \tag{7}$$

$$h = \tan(i/2)\cos\Omega \tag{8}$$

$$k = \tan(i/2)\sin\Omega \tag{9}$$

$$L = \Omega + \omega + \nu \tag{10}$$

The equations of motion of a thrusting spacecraft in an inverse square gravity field in terms of the modified equinoctial orbit elements[18,19] are

$$\dot{p} = (2p/w)\sqrt{(p/\mu)}\Delta_\theta \tag{11}$$

$$\dot{f} = \sqrt{(p/\mu)}\{\Delta_r \sin L + [(w+1)\cos L + f](\Delta_\theta/w) - (h\sin L - k\cos L)(g\Delta_h/w)\} \tag{12}$$

$$\dot{g} = \sqrt{(p/\mu)}\{-\Delta_r \cos L + [(w+1)\sin L + g](\Delta_\theta/w) + (h\sin L - k\cos L)(f\Delta_h/w)\} \tag{13}$$

$$\dot{h} = \sqrt{(p/\mu)}\left(s^2\Delta_h/2w\right)\cos L \tag{14}$$

$$\dot{k} = \sqrt{(p/\mu)}\left(s^2\Delta_h/2w\right)\sin L \tag{15}$$

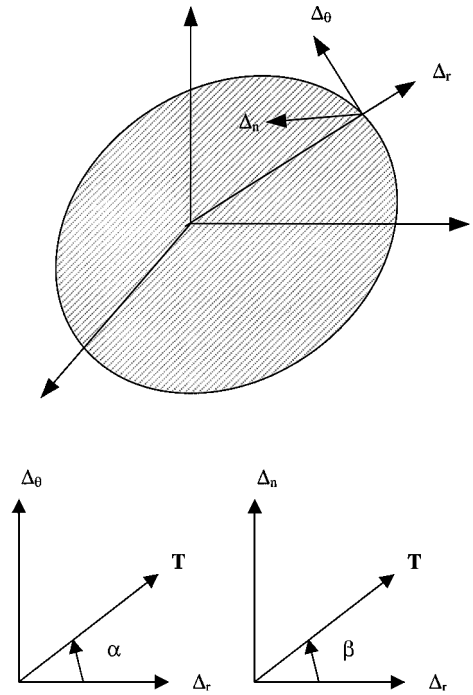

Fig. 1 Thrust vector and angle definitions.

$$\dot{L} = \sqrt{\mu p}(w/p)^2 + \frac{1}{w}\sqrt{(p/\mu)}(h\sin L - k\cos L)\Delta_h \tag{16}$$

$$\dot{m} = -T/c \tag{17}$$

where $w = 1 + f\cos L + g\sin L$; $s^2 = 1 + h^2 + k^2$. Introducing a nondimensional form of the mass $\eta = m/m_0$, Eq. (17) can be replaced by

$$\dot{\eta} = -(T/m_0)(1/c) \tag{18}$$

The thrust vector $\boldsymbol{T}$ is computed using two angles α and β, which represent the in-plane and out-of-plane components of the thrust direction, respectively, that is,

$$\boldsymbol{T} = T\begin{Bmatrix}\sin(\alpha)\cos(\beta)\\ \cos(\alpha)\cos(\beta)\\ \sin(\beta)\end{Bmatrix} = \begin{Bmatrix}\Delta_r\\ \Delta_\theta\\ \Delta_h\end{Bmatrix} \tag{19}$$

The geometry of the thrust angles is shown in Fig. 1.

Results

Cases where a spacecraft is transferred from low Earth orbit (LEO) to geosynchronous Earth orbit (GEO), LEO to medium Earth orbit (MEO), and LEO to high Earth orbit (HEO) while maximizing the final mass are solved. The LEO, GEO, MEO, and HEO conditions used for this analysis are shown in Table 1. The LEO and GEO values are representative of these orbits. The MEO is a global-positioning-system-type orbit. The HEO is a representative Molniya orbit. Also, different spacecraft configurations were assumed. These configurations had varying thrust accelerations (TA) ranging from 10 to 10^{-2} N/kg (approximately 1–10^{-3} g, respectively) and were incremented in orders of magnitude, that is, the thrust accelerations considered were 10, 1, 10^{-1}, and 10^{-2} N/kg. The variations resulted in a total of 12 orbit transfer cases. For all cases a burn-coast-burn thrusting structure was a priori determined for the transfer trajectories that duplicate the burn structure presented by Spencer.[12]

Each of the optimal orbit transfer cases was solved assuming each of the thrust levels, and the results for the maneuvers were analyzed. The cases were compared on the basis of their effective velocity change ΔV_{eff} according to the analysis developed by Spencer,[12] which produces the relation given by

$$\Delta V_{\text{eff}} = -\left(\frac{T}{m_0}\right)\left\{\frac{\ell n[\eta(t_i)] - \ell n[\eta(t_{i-1})]}{\eta(t_i) - \eta(t_{i-1})}\right\}\Delta t_i \tag{20}$$

where η is the ratio of mass relative to the initial mass m_0, that is, $\eta(t_i) = m_i/m_0$. The advantage of using this methodology is that it allows for a direct comparison of results generated by various thrust acceleration levels. Spacecraft mass can be derived from Eq. (20); however, this result was not produced because a nondimensional mass was included in the differential equations of motion (the mass ratio η was calculated during the solution of the simultaneous differential equations of motion).

Using Eq. (20), the results are shown in Table 2 for the LEO to GEO transfers, Table 3 for the LEO to MEO transfers, and Table 4 for the LEO to HEO transfers. In each transfer type the highest thrust acceleration (10 N/kg, which is approximately 1 g) results in a transfer that nearly achieves the performance one would expect from using a high-thrust, impulsive approximation to the transfer maneuvers, that is, the burn duration is small when compared to the coast arc, which is the basic assumption made when assuming an impulsive approximation. The total transfer time is only a few hours. For a case that results in a TA of 1 N/kg, the ΔV_{eff} and transfer time is slightly higher. As the TA decreases, the ΔV_{eff} and transfer time increases. With a 10^{-1} N/kg TA the ΔV_{eff} required is 20–25% more for the LEO-to-GEO and LEO-to-MEO cases. The three-dimensional trajectory for this case is shown in Fig. 2a. Here, as in all figures, the thick line represents a burn arc, whereas the thin

Table 1 LEO and GEO/MEO/HEO conditions for transfer trajectories

Orbital element	LEO	GEO	MEO	HEO
Semimajor axis, km	7,003	42,287	26,560	26,578
Eccentricity	0	0	0	0.73646
Inclination, deg	28.5	0	54.7	63.435
Right ascension of the ascending node, deg	0	0	0	0
Argument of perigee, deg	0	0	0	0
Mean anomaly, deg	Free	Free	Free	Free

Table 2 LEO-to-GEO transfer results

Initial thrust acceleration, N/kg	Effective ΔV, m/s			Total transfer time, hours
	First burn	Second burn	Total	
10^1	2366	1761	4127	5.40
10^0	2592	1716	4308	6.06
10^{-1}	4079	1088	5167	18.32
10^{-2}	5698	——	5698	149.59

Table 3 LEO-to-MEO transfer results

Initial thrust acceleration, N/kg	Effective ΔV, m/s			Total transfer time, hours
	First burn	Second burn	Total	
10^1	2008	1856	3863	3.06
10^0	2137	1834	3970	3.60
10^{-1}	3717	1014	4731	14.56
10^{-2}	5122	——	5122	135.23

Table 4 LEO-to-HEO transfer results

Initial thrust acceleration, N/kg	Effective ΔV, m/s			Total transfer time, hours
	First burn	Second burn	Total	
10^1	2434	836	3271	6.03
10^0	2666	890	3555	6.55
10^{-1}	4146	1125	5271	18.59
10^{-2}	6109	——	6109	159.75

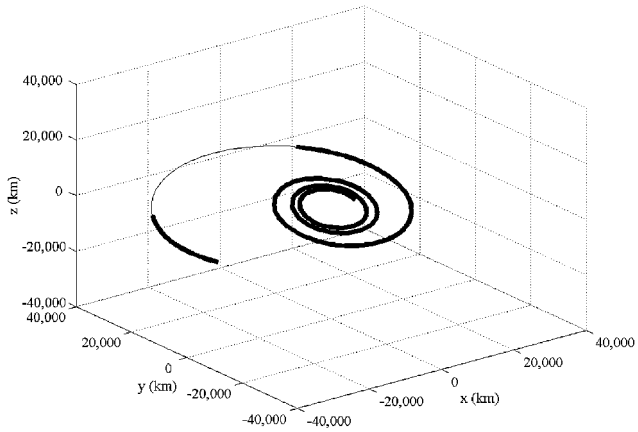

Fig. 2a LEO-to-GEO transfer with initial thrust acceleration of 10^{-1} N/kg.

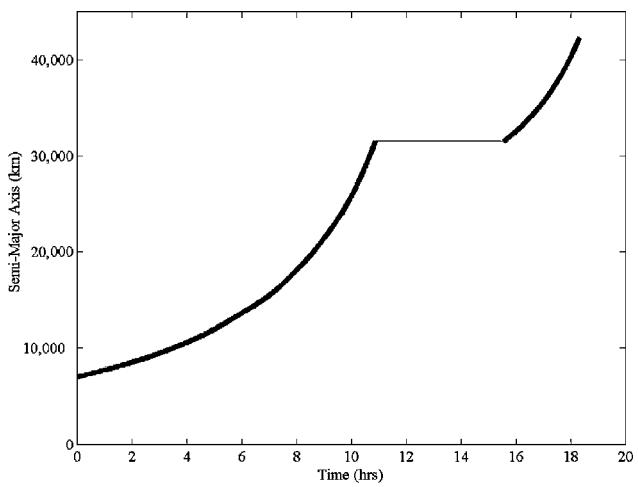

Fig. 2b LEO-to-GEO transfer with initial thrust acceleration of 10^{-1} N/kg.

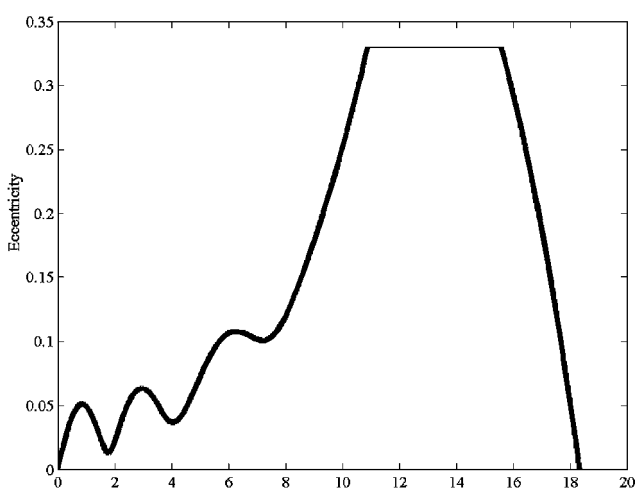

Fig. 2c LEO-to-GEO transfer with initial thrust acceleration of 10^{-1} N/kg.

line represents a coast arc. The semimajor axis, eccentricity, and inclination time histories for this LEO-to-GEO transfer case are shown in Figs. 2b–2d, respectively. The majority of the change in semimajor axis is performed during the first burn. During this burn, the eccentricity is increased to its maximum value of approximately 0.33, and the initial inclination is reduced by nearly 10 deg. During the final burn, the semimajor axis is increased to correspond to GEO while the eccentricity and inclination are both reduced to zero.

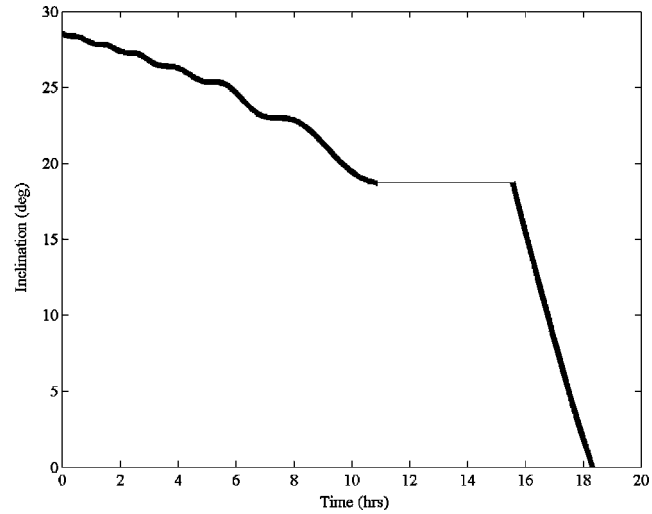

Fig. 2d LEO-to-GEO transfer with initial thrust acceleration of 10^{-1} N/kg.

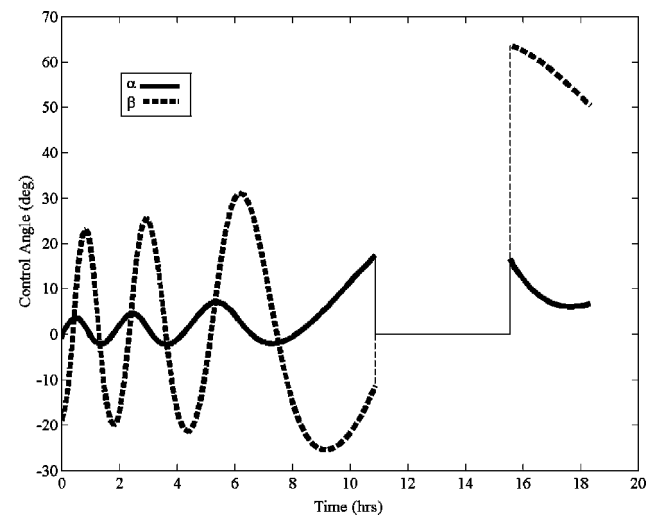

Fig. 2e LEO-to-GEO transfer with initial thrust acceleration of 10^{-1} N/kg.

For this transfer the thrust pointing direction angles are shown in Fig. 2e. The figures clearly indicate that the optimal thrusting profiles include a significant amount of inclination reduction during the first burn. The total transfer time is just over 18 h.

For the LEO-to-MEO case with 10^{-1} N/kg TA, the three-dimensional view of the trajectory for the transfer is shown in Fig. 3a. The semimajor axis, eccentricity, and inclination time histories for the LEO-to-MEO transfer are shown in Figs. 3b–3d, respectively. The majority of the change in semimajor axis is performed during the first burn. During this burn, the eccentricity is increased to its maximum value of just over 0.2, and the inclination is increased from its initial value by approximately 14 deg. During the final burn, the semimajor axis is increased to correspond to the final MEO value specified while the eccentricity is reduced to zero and the final desired inclination is achieved. For this transfer the thrust-pointing direction angles are shown in Fig. 3e. In this case the out-of-plane (β) profile takes on the appearance of opposite sign to the LEO-to-GEO thrusting pointing angle profile shown in Fig. 2e. This result is in keeping with the difference in change in inclination that must be performed between the two cases. The total transfer time for this case is approximately 14.5 h, as shown in Table 3.

For the LEO-to-HEO case with 10^{-1} N/kg TA, the ΔV_{eff} is 60% more than the 10 N/kg TA case. The trajectory, state time histories, and control profiles are shown in Figs. 4a–4e. The three-dimensional view is shown in Fig. 4a. The semimajor axis is shown in Fig. 4b.

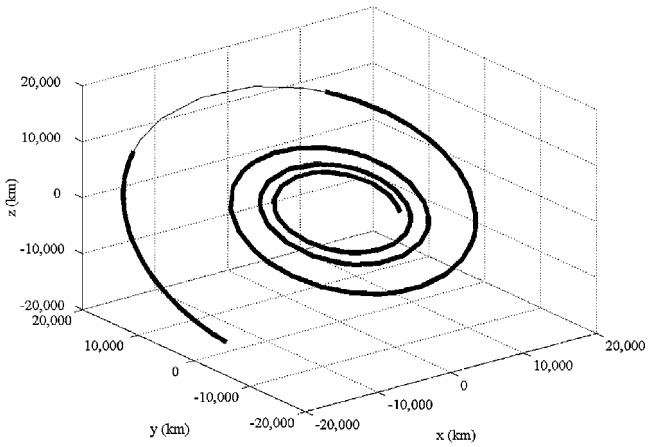

Fig. 3a LEO-to-MEO transfer with initial thrust acceleration of 10^{-1} N/kg.

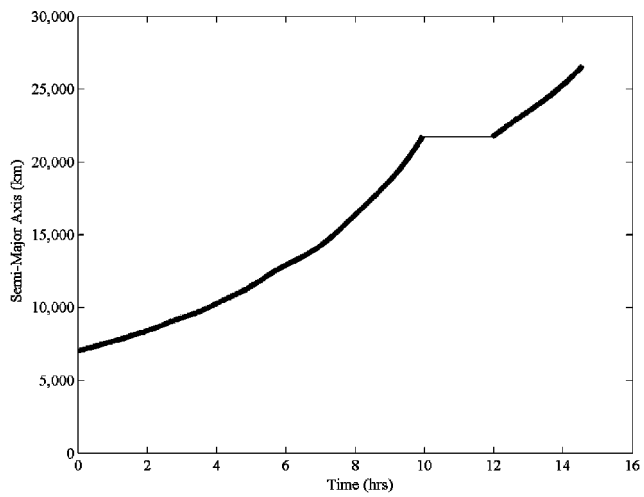

Fig. 3b LEO-to-MEO transfer with initial thrust acceleration of 10^{-1} N/kg.

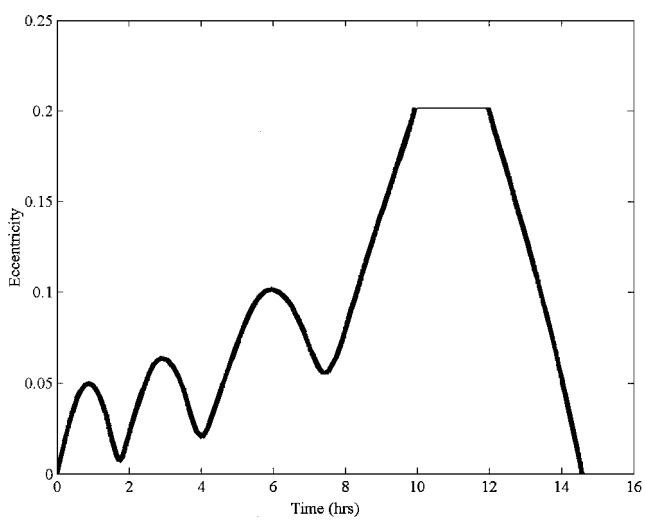

Fig. 3c LEO-to-MEO transfer with initial thrust acceleration of 10^{-1} N/kg.

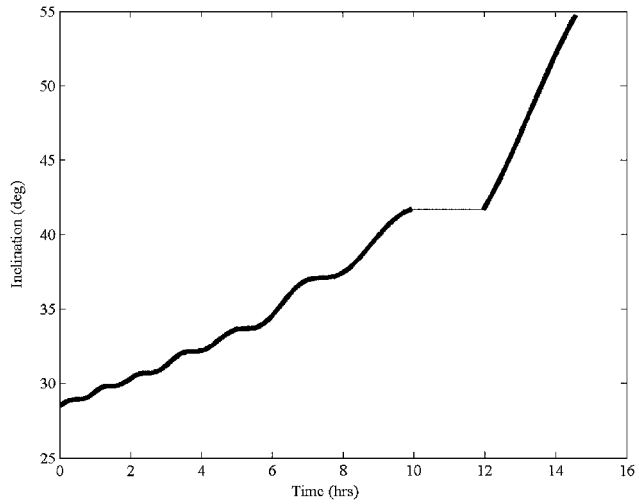

Fig. 3d LEO-to-MEO transfer with initial thrust acceleration of 10^{-1} N/kg.

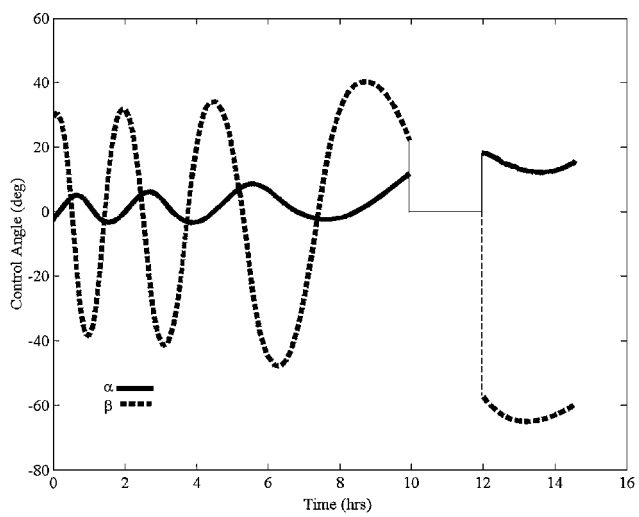

Fig. 3e LEO-to-MEO transfer with initial thrust acceleration of 10^{-1} N/kg.

As can be seen, the semimajor axis is increased during the first burn above the final value specified for this case. During the last burn, lowering the perigee location decreases the semimajor axis. The result is an increase in eccentricity to the final value specified (Fig. 4c). At the same time the majority of the inclination change takes place during the last burn, as can be seen in Fig. 4d. As shown in Fig. 4e, the in-plane thrust direction angle (α) is near 180 deg, which is approximately in the antivelocity direction. This thrust direction profile corresponds to the state time histories. The total transfer time for this case is approximately 18.6 h.

Finally, cases with a TA of 10^{-2} N/kg were analyzed for each transfer type. In each of these cases, the resulting optimal transfer exhibited no coast. Therefore, the only burn is listed as the first burn in the Tables 3–5. The resulting transfer takes on the spiral shape with increasing radius as is expected for low-thrust trajectories. The ΔV_{eff} for the LEO-to-GEO and LEO-to-MEO transfer type are approximately 35% greater than the corresponding transfer types with a TA of 10 N/kg, and the LEO-to-HEO transfer type is approximately 85% more than the corresponding transfer with a TA of 10 N/kg.

Analytical Comparison

A comparison was made between the results obtained by Spencer[12] for a LEO-to-GEO transfer and analogous results obtained here using the DHOC7 method. The primary goal of Spencer's work was to minimize the propellant usage for a given transfer. To accomplish this goal, assuming that the propellant usage rate is constant during a burn, the burn times are minimized. To minimize the burn time for a given maneuver, the time rate of change of a particular orbital parameter that is used to govern the burn is maximized. For the first burn thrusting in the orbit plane is performed to increase the apogee radius approximately to the desired circular GEO radius value. The in-plane (α) motion of the thrust direction is determined to maximize the rate of change of the semimajor axis, that is, da/dt is maximized during the first burn.

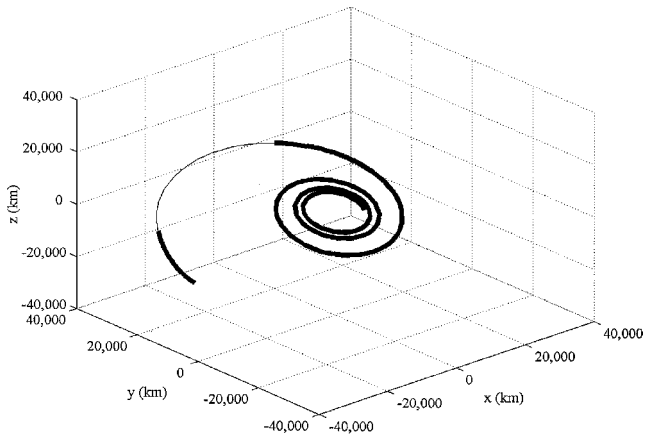

Fig. 4a LEO-to-HEO transfer with initial thrust acceleration of 10^{-1} N/kg.

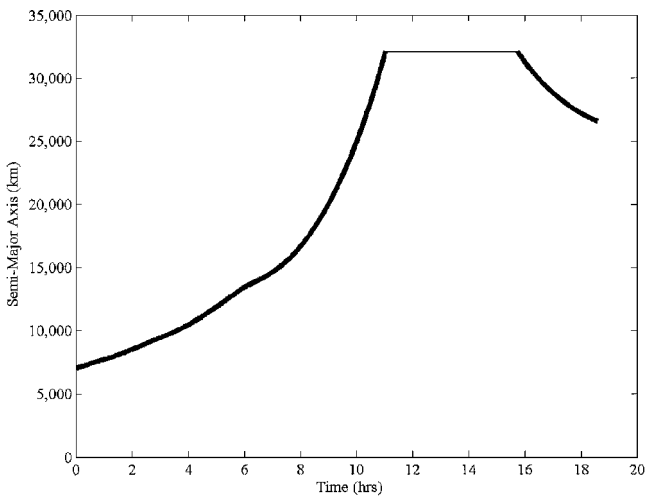

Fig. 4b LEO-to-HEO transfer with initial thrust acceleration of 10^{-1} N/kg.

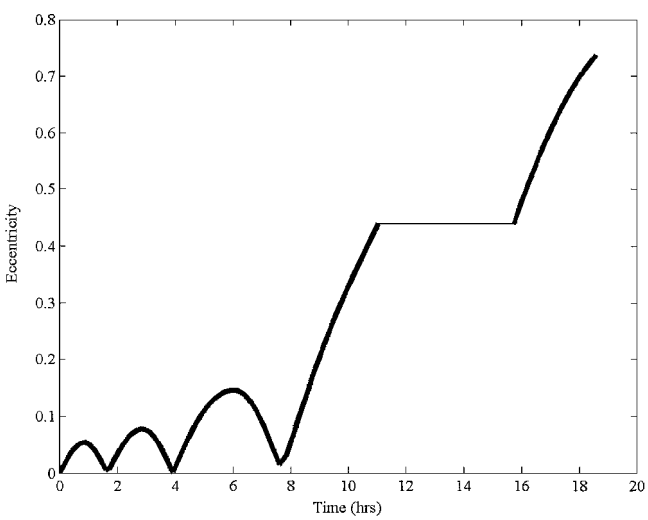

Fig. 4c LEO-to-HEO transfer with initial thrust acceleration of 10^{-1} N/kg.

During the first burn, there exists no out-of-plane component of the thrust vector. The formulation for maximizing $\mathrm{d}a/\mathrm{d}t$ during the first burn is described in detail by Spencer.[12] Following the first burn, a coast is initiated that lasts until a second burn begins. During the second burn, the inclination of the spacecraft's orbit is the first change from the initial value to the desired final value, and then the orbit is circularized to correspond to GEO. The first part of the second burn that changes inclination is designed to minimize the burn time

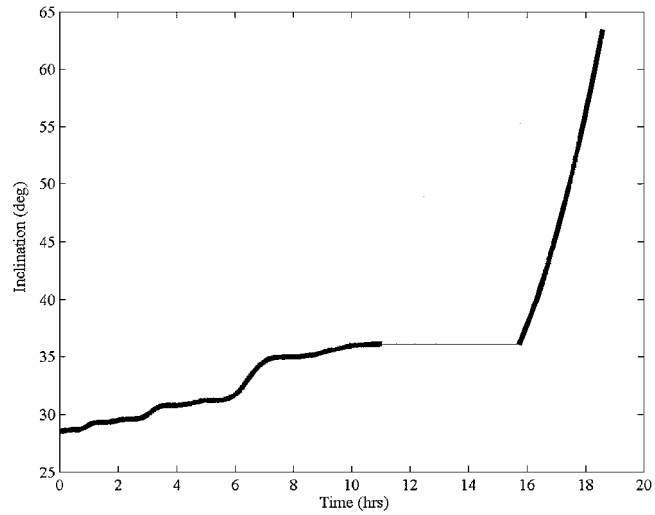

Fig. 4d LEO-to-HEO transfer with initial thrust acceleration of 10^{-1} N/kg.

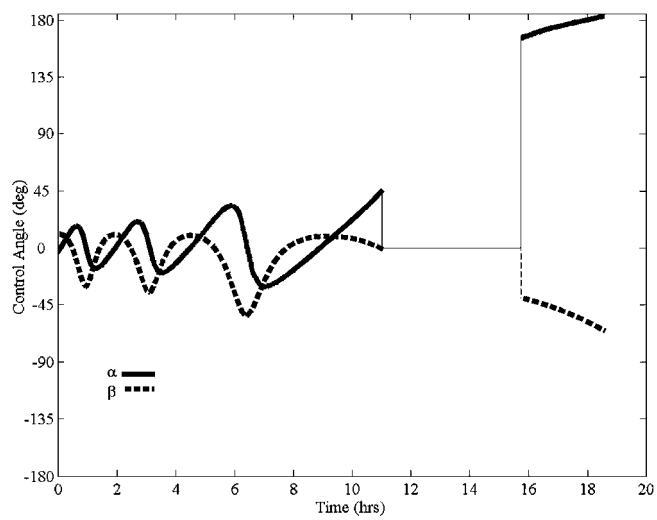

Fig. 4e LEO-to-HEO transfer with initial thrust acceleration of 10^{-1} N/kg.

by maximizing the change in inclination, that is, $|\mathrm{d}i/\mathrm{d}t|$ is maximized. The result is that the out-of-plane thrust angle (β) is near either ± 90 deg, where the sign ambiguity is resolved by whether one wishes to increase or decrease the inclination. The inclination change maneuver is centered about apogee. For example, if the inclination burn is determined to take Δt, the inclination maneuver begins $\frac{1}{2}\Delta t$ prior to apogee passage. The second part of the second burn circularizes the spacecraft's orbit at GEO. The in-plane thrust-pointing direction is chosen such that the time rate of change of the apogee radius is zero, that is, $|\mathrm{d}r_a/\mathrm{d}t| \equiv 0$, throughout the duration of the circularization maneuver. As in the first burn, the out-of-plane component of the thrust vector is zero.

Spencer used his orbit transfer method to examine various LEO-to-GEO transfers with a range of TA values. For all cases he assumed a specific impulse of 1000 s. A transfer case with a TA of 10^{-1} N/kg was analyzed by both Spencer's method and DHOC7, assuming the same thrust structure. A case named "3 Burns-Separate Controls" is directly analogous to the method developed by Spencer. Here, the first and third burns are forced to raise the orbit, while the second burn rotates the orbit plane (zeroing out the inclination). As shown in Table 5, the difference in performance between these two cases is only 2.4%. Thus, Spencer's method provides near-optimal performance assuming his thrusting strategy. The semimajor axis, eccentricity, and inclination time histories are shown in Figs. 5–7, respectively. The only significant difference between Spencer's results and the 3-Burn result appears to be in the timing of the start of the

Table 5 Comparison of LEO-to-GEO transfers methods

Case	Effective ΔV, m/s				Change in total effective ΔV
	First burn	Second burn	Third burn	Total	
Spencer's results	3785	1237	782	5804	——
3 Burns—separate controls	3751	1244	674	5668	2.40%
2 Burns—combined second burn	3749	1499	——	5248	10.6%
2 Burns—optimized thrust directions	3944	1133	——	5077	14.3%

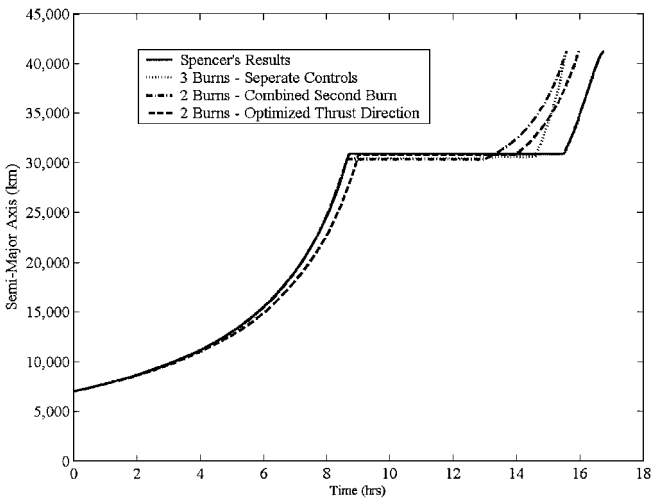

Fig. 5 Comparison of semimajor axis time histories.

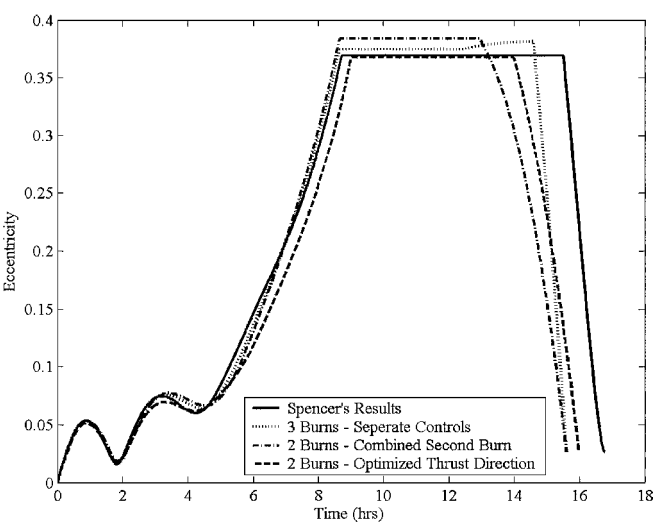

Fig. 6 Comparison of eccentricity time histories.

second burn to remove the inclination. The DHOC7 solution begins this burn approximately one hour prior to Spencer's method. This can be explained by the a priori choice of second burn time initialization. Next, a 2-burn case where the inclination and circularization burns are combined into one burn is analyzed (and labeled "2 Burns–Combined Second Burn"). The performance increase over Spencer's case is 10.6%. This is expected, because combining the second and third burns together can change the semimajor axis and the inclination together more efficiently than alone. Finally, a 2-burn case where the first burn is allowed to perform inclination maneuvers as

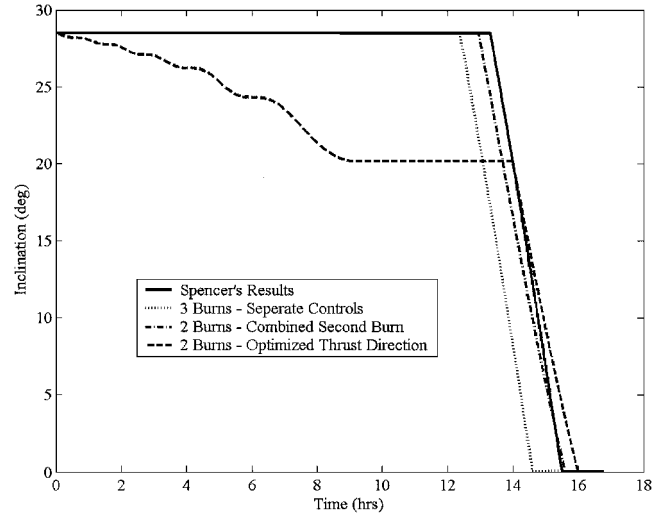

Fig. 7 Comparison of inclination time histories.

well as a combined second burn (labeled as "2 Burns–Optimization Thrust Direction") results in a 14.3% increase in performance over Spencer's method, as this method is considered to be the optimal, two-burn, three-dimensional solution.

Conclusions

This study has established the utility of the DHOC7 method for solving a wide variety of Earth-orbit transfers. In addition, the method was compared with a previously developed method by Spencer. This analysis shows that Spencer's method is capable of producing near-optimal orbit transfers with the a priori specification for the burn-coast-burn thrusting structure that he assumed. However, when this a priori specification is dropped the added complexity of the problem requires solution of the problem using numerical techniques, like DHOC7. Nevertheless, approximate solutions can provide useful results without the need for the cumbersome computation found in numerical methods. The HOC7 method was robust for the higher thrust cases. However, for the very low-thrust cases problems with execution time and convergence made this a cumbersome problem to solve. Using the analytical methods yielded solutions for a wide variety of acceleration levels, although while it did not produce the optimal solution, the solution was nearly optimal and was obtained quickly.

Future work on this problem could include adding additional forces such as Earth geopotential effects, atmospheric drag, solar radiation pressure, and luni-solar perturbations. Such disturbances can easily be included in the direct collocation method.

Acknowledgment

This work was sponsored by the U.S. Air Force, Air Force Material Command, Air Force Research Laboratory Space Vehicles Directorate (AFRL/VS), Kirtland AFB, New Mexico.

References

[1] Dickerson, W. D., and Smith, D. B., "Trajectory Optimization for Solar-Electric Powered Vehicles," AIAA Paper 67-583, Aug. 1967.

[2] Sauer, C. G., "Optimization of a Solar-Electric-Propulsion Planetary Orbiter Spacecraft," American Astronautical Society, Paper 68-104, Sept. 1968.

[3] Oglevie, R. E., Andrews, P. D., and Jasper, T. P., "Attitude Control Requirements for an Earth Orbital Solar Electric Propulsion Stage," AIAA Paper 75-353, March 1975.

[4] Avila, E. R., "ELITE Program Overview," AIAA Paper 92-1559, March 1992.

[5] Brusch, R. G., and Vincent, T. L., "Low-Thrust, Minimum Fuel, Orbit Transfers," *Acta Astronautica*, Vol. 16, No. 2, 1971, pp. 65–73.

[6] Edelbaum, T. N., "Propulsion Requirements for Controllable Satellites," *ARS Journal*, Vol. 32, No. 8, 1961, pp. 1079–1089.

[7] Redding, D. C., "Optimal Low-Thrust Transfers to Geosynchronous Orbit," Stanford Univ. Guidance and Control Lab., Rept. SUDAAR 539, Stanford, CA, Sept. 1983.

[8]Alfano, S., "Low-Thrust Orbit Transfer," M.S. Thesis, Dept. of Aeronautics and Astronautics, Air Force Inst. of Technology, AFIT/GA/AA/82D-2, Wright–Patterson AFB, OH, Dec. 1982.

[9]Bauer, T. A., "Near-Optimum Low-Thrust Transfer in Semimajor Axis and Eccentricity," American Astronautical Society, Paper 92-134, Feb. 1992.

[10]Stewart, D. J., and Melton, R. G., "Approximate Analytic Representation for Low-Thrust Trajectories," American Astronautical Society, Paper 91-512, Aug. 1991.

[11]Hargraves, C. R., and Paris, S. W., "Direct Trajectory Optimization Using Nonlinear Programming and Collocation," *Journal of Guidance, Control, and Dynamics*, Vol. 10, No. 4, 1987, pp. 338–342.

[12]Spencer, D. B., "An Analytical Solution Method for Near-Optimal Continuous-Thrust Orbit Transfers," Ph.D. Dissertation, Dept. of Aerospace Engineering Sciences, Univ. of Colorado, Boulder, CO, 1994.

[13]Herman, A. L., "Improved Collocation Methods with Application to Direct Trajectory Optimization," Ph.D. Dissertation, Dept. of Aeronautical and Astronautical Engineering, Univ. of Illinois at Urbana–Champaign, IL, Sept. 1995.

[14]Bryson, A. E., Jr., *Dynamic Optimization*, Addison Wesley Longman, Reading, MA, 1999.

[15]Bryson, A. E., Jr., and Ho, Y.-C., *Applied Optimal Control*, Hemisphere, Washington, DC, 1975.

[16]Kechichian, J. A., "Minimum-Time Low-Thrust Rendezvous and Transfer Using Epoch Mean Longitude Formulation," *Journal of Guidance, Control, and Dynamics*, Vol. 22, No. 3, 1999, pp. 421–432.

[17]Gill, P. E., Murray, W., and Saunders, M. A., "User's Guide for SNOPT 5.3: A FORTRAN Package for Large-Scale Nonlinear Programming," Stanford Business Software, Inc., Palo Alto, CA, 1998.

[18]Walker, M. J. H., Ireland, B., and Owens, J., "A Set of Modified Equinoctial Orbit Elements," *Celestial Mechanics*, Vol. 36, No. 4, 1985, pp. 409–419.

[19]Betts, J. T., "Optimal Interplanetary Orbit Transfers by Direct Transcription," *Journal of Astronautical Sciences*, Vol. 42, No. 3, 1994, pp. 247–268.